Subcarrier-based Processing for Clutter Rejection in CP-OFDM Signal-based Passive Radar Using SFN Configuration

Yi Jian-xin Wan Xian-rong* Zhao Zhi-xin Cheng Feng Ke Heng-yu
(*Radio Propagation Laboratory, School of Electronic Information, Wuhan University, Wuhan* 430072, *China*)

Abstract: Clutter rejection is a key technique used by passive radars for target detection. Especially when using Single Frequency Network (SFN) configuration, the multipath clutter and ground clutter increase several times more than during a single illuminator situation, which means that the clutter extends in both the spatial and temporal dimensions. The high amount of clutter occupies numerous degrees of freedom when conventional spatial or temporal processing is used, leading to a large array requirement, a huge computational cost, or even a complete failure. This paper investigates a novel subcarrier-based processing technique that is tailored for Orthogonal Frequency Division Multiplex (OFDM) modulation with a Cyclic Prefix (CP-OFDM) to avoid the above-mentioned predicament. The algorithm principle is initially illustrated and followed by a discussion about the unique characteristics of Subcarrier-based Spatial Adaptive Processing (SSAP), which include the Doppler response and its unusual main-lobe clutter case. Then, the robustness is researched by evaluating the performance under relaxed basic assumptions. The conclusions are demonstrated by conducting test using simulated and real datasets.

Key words: Passive radar; Single Frequency Network (SFN); Cyclic Prefix OFDM (CP-OFDM) modulation; Subcarrier-based processing
CLC index: TN958.97
DOI: 10.3724/SP.J.1300.2013.13030

单频网 CP-OFDM 信号外辐射源雷达的分载波杂波抑制方法

易建新 万显荣 赵志欣 程 丰 柯亨玉
(武汉大学电子信息学院电波传播实验室 武汉 430072)

摘 要：杂波抑制是外辐射源雷达目标检测的一项关键技术。尤其在单频网配置下，多径杂波和地杂波相对于单发射站情况成倍增长，造成其在空域和时域均具更大扩展，使得传统杂波处理方法面临新的困难。该文研究了一种新的分载波杂波抑制方法，该方法针对带循环前缀的正交频分复用信号(CP-OFDM)所设计，能较好克服单频网配置给杂波抑制引入的新问题。文章首先阐述了该方法的原理，接着展示了其有别于传统方法的特性，包括分载波空域处理的多普勒响应和全新的主瓣杂波问题，然后从理论上研究了该方法的鲁棒性，仿真和实测处理结果验证了该文方法的有效性。

关键词：外辐射源雷达；单频网；CP-OFDM 调制；分载波处理
中图分类号：TN958.97 **文献标识码**：A **文章编号**：2095-283X(2013)01-0001-13

1 Introduction

Passive Coherent Location (PCL) or Passive Covert Radar, short passive radar, is an emerging and highly promising technology[1−9], which may be used in many application areas in future[10−15]. Passive radar exploits the availability of so called "illuminators-of-opportunity" in the environment for the illumination of targets. The key-benefits of passive radar are, apart from its covert operation, the low-cost nature due to saving on expensive transmitters as well as detection of low-altitude and/or stealthy targets. Nowadays broadcast transmissions are changing more and more from analogue to digital. Passive radar research is focusing on the use of digital broadcast transmitters for illumination accordingly.

Manuscript received March 20, 2013; revised March 20, 2013. Published online March 27, 2013.
Supported by the National Natural Science Foundation of China (No. 41074116, 41106156, 61271400, and 60971101).
*Corresponding author: Wan Xian-rong.
E-mail: xrwan@whu.edu.cn.

Among the digital transmissions, most of modern digital TV and broadcast systems adopt Single Frequency Network (SFN) technology, such as DVB-T[16], DAB[10], CMMB (China Mobile Multimedia Broadcasting)[6], and so on. In SFN each illuminator transmits the same content at the same frequency simultaneously. From the perspective of broadcast and communication, SFN is an efficient coverage approach since a group of illuminators constitutes a network with a wide range of coverage but only occupies one work bandwidth. Thus, it is a kind of power and frequency saving system. Nevertheless, owing to the same waveform in all the illuminators, the direct-path signal of each illuminator is equivalent to multipath clutter in terms of correlation output. It indicates that the SFN itself constitutes a multipath channel even ignoring the external reflection and scattering. The direct-path signals are strong multipath signal. In addition respective multipath clutters and ground clutters, the received clutters possess a greater extension in both spatial and temporal dimensions compared with the single illuminator situation. In this case, conventional temporal methods, such as in Refs. [17,18], would consume much more filter order, leading to computation explosion. With respect to traditional Spatial Adaptive Processing (SAP), like in Refs. [19,20], as the broadcasting waveform is not dedicated for radar applications, there is still interaction between two far separated clutters in range-Doppler domain. Therefore, traditional SAP is prone to be overloaded under small or medium array.

In the face of these difficulties, new methods must be explored. Fortunately, the multipath processing technique in communication provides us the inspiration. Modern digital TV systems usually adopt OFDM (Orthogonal Frequency Division Multiplex) modulation. In particular, a Cyclic Prefix (CP) is inserted between each two useful OFDM symbols to prevent Inter-Symbols Interferences (ISI) and keep the inter-carrier orthogonality under multipath environment. It can be called CP-OFDM modulation. Then the influence of multipath signals could be compensated with channel equalization in useful symbol window. It is interesting to note that the inter-carrier orthogonality under multipath environment means that the multipath signals are coherent with each other in each subcarrier. The coherence feature indicates that the clutters only occupy one degree of freedom in subcarrier domain. Inspired from this, we maybe achieve clutter rejection more easily in subcarrier domain.

Actually, the idea of Subcarrier-based Spatial Adaptive Processing (SSAP) is first conceived in Ref. [21] and has been preliminarily discussed in Ref. [22]. Theoretical analyses and simulation results have proved the assertion that it can save degree of freedom by beamforming in subcarrier domain. In addition, the thought of SSAP has been extended in Ref. [23] by combining the temporal cancellation technique. It shows that Subcarrier-based Temporal Rejection (STR) approach can effectively reduce computational complexity compared with the conventional temporal approaches. Nevertheless, the characteristics of SSAP and STR have not been thoroughly discussed and the assumptions involved therein could be violated in real-life environment. So their characteristics and robustness are further investigated in this paper to promote its applications.

SSAP and STR are subsumed into the frame of subcarrier-based processing in this paper. As mentioned above, the key point of subcarrier-based processing is the coherence among clutters in subcarrier domain. It is actually a coherent clutter rejection problem which presents several unique features. Specifically, we investigate its Doppler response that tells us how many samples should be selected, and the main-lobe clutter case of SSAP which is different from the one in conventional SAP. Furthermore, as the assumptions involved in strict theoretical derivation could be violated in real-life environment, the sensitivity of the algorithm to Carrier Frequency Offset (CFO) and excessive channel delay extension is explored. The robustness study will reveal the algorithm's performance in real-life environment.

The paper is organized as follows. Section 2 introduces the SFN signal model and the principle

of subcarrier-based processing. The unusual characteristics are presented in Section 3. Then the robustness is discussed in Section 4. Section 5 gives the simulated and real-life data results to verify the above discussions. Finally conclusions are drawn in Section 6.

2 Principle of Subcarrier-based Processing

2.1 SFN signal model

Passive radar is usually equipped with two receiving channels: reference and surveillance channels. The reference channel serves as a source of the original transmitted signal. The other channel, or digitally formed beam, is looking towards the area of interest and is a source of the surveillance (echo) signal. Assume that the ground clutters and multipath clutters can be represented as a collection of multiple stationary point scatters. These clutters usually possesses zero Doppler frequency (at least nearly zero Doppler frequency), while the echoes of moving targets are characterized by nonzero Doppler frequency. If there are P transmitters in the SFN, then the complex envelope of the surveillance signal is given by

$$\begin{aligned} s_{\text{surv}}(t) = &\left[\sum_{p=1}^{P} A_p d(t-t_p) + \sum_{p=1}^{P}\sum_{n=1}^{N_c} c_{p,n} d(t-\tau_{p,n}^{c}) \right. \\ &\left. + \sum_{p=1}^{P}\sum_{m=1}^{N_t} \alpha_{p,m} d(t-\tau_{p,m}) \exp\left(j2\pi f_{p,m}^{D} t\right)\right] \\ &\cdot \exp\left(j2\pi f_{\text{CFO}} t\right) + w_{\text{surv}}(t) \end{aligned} \tag{1}$$

where $d(t-t_p)$ is the direct-path signal of p-th transmitter (without loss of generality, assume the first transmitter is the nearest one, $t_1 = 0$), A_p is the corresponding complex amplitude; $c_{p,n}, \tau_{p,n}^{c}$ are the complex amplitude and the delay (with respect to the first path) of the n-th stationary point scatterer ($n = 1,\cdots,N_c$), respectively; $\alpha_{p,m}, \tau_{p,m}$, $f_{p,m}^{D}$ are the complex amplitude, the delay and the Doppler frequency of the m-th target ($m = 1,\cdots,N_t$), respectively; f_{CFO} is CFO between the transmitter and receiver; $w_{\text{surv}}(t)$ is the thermal noise.

Obviously, the clutters under SFN configuration increase to P times of the single transmitter case. In fact, there is no much difference between the direct-path signals of SFN transmitters and the reflections of fixed scatterers. We call them clutters without distinction under unambiguous situation. For description convenience, we recast Eq. (1) as follows

$$\begin{aligned} s_{\text{surv}}(t) = &\left[c_1 d(t) + \sum_{n=2}^{M_c} c_n d(t-\tau_n^{c}) \right. \\ &\left. + \sum_{m=1}^{M_t} \alpha_m d(t-\tau_m) \exp\left(j2\pi f_m^{D} t\right)\right] \\ &\cdot \exp\left(j2\pi f_{\text{CFO}} t\right) + w_{\text{surv}}(t) \end{aligned} \tag{2}$$

where $M_c = P(N_c + 1)$ and $M_t = PN_t$. The maximum value of τ_n^{c} denotes the channel delay extension.

For the sake of argument, we further established the array signal model to investigate spatial processing. The temporal processing can be conducted on the signal of each array element or each beamformer output. Assuming the CFO has been compensated, *i.e.* $f_{\text{CFO}} = 0$, the array signal model based on model Eq. (2) can be expressed as

$$\begin{aligned} \boldsymbol{s}(t) = &\boldsymbol{a}(\theta_1^{c}) c_1 d(t) + \sum_{n=2}^{M_c} \boldsymbol{a}(\theta_n^{c}) c_n d(t-\tau_n^{c}) \\ &+ \sum_{m=1}^{M_t} \boldsymbol{a}(\theta_m^{t}) \alpha_m d(t-\tau_m) \exp\left(j2\pi f_m^{D} t\right) + \boldsymbol{w}(t) \end{aligned} \tag{3}$$

where $\boldsymbol{s}(t) = \left[s_{\text{surv}}^{1}(t), s_{\text{surv}}^{2}(t), \cdots, s_{\text{surv}}^{N}(t)\right]^{\text{T}}$ is the receiving signal vector, $s_{\text{surv}}^{i}(t)$ is the signal of the i-th antenna, superscript "T" denotes transpose operation, N is the number of array antennas; $\boldsymbol{a}(\theta)$ is the array steering vector with dimension $N \times 1$; $\boldsymbol{w}(t) = \left[w_{\text{surv}}^{1}(t), w_{\text{surv}}^{2}(t), \cdots, w_{\text{surv}}^{N}(t)\right]^{\text{T}}$ is the thermal noise vector.

According to the CP-OFDM principle, the direct signal can be written as

$$d(t) = \sum_{l=-\infty}^{+\infty} \sum_{k=0}^{K-1} C_{l,k} \psi_{l,k}'(t) \tag{4}$$

with

$$\begin{aligned} &\psi_{l,k}'(t) = g_k'(t - lT_S), \\ &g_k'(t) = \begin{cases} \exp\left(j2\pi f_k t\right), & -T_{\text{cp}} \le t < T_u \\ 0, & \text{elsewhere} \end{cases} \end{aligned} \tag{5}$$

where T_u is the duration of useful symbol, T_{cp} is the duration of the CP, $T_s = T_u + T_{\text{cp}}$ is the duration of one OFDM block (the typical structure of CP-OFDM modulation is shown in Fig. 1), $C_{l,k}$ represents the transmitted information of l-th OFDM block at k-th subcarrier and the subcarriers

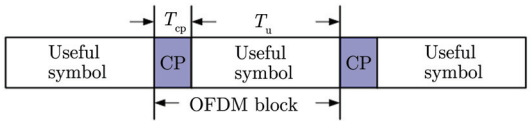

Fig. 1 The typical structure of CP-OFDM modulation

$f_k = k / T_u$. Direct signal is used as reference sample in temporal cancellation and matched filtering. It is assumed to have been obtained from the reference channel.

2.2 Principle of subcarrier-based processing

As we all know, the good anti-interference performance of CP-OFDM modulation for communication purpose attributes to the insertion of CP. The CP is usually assumed to be greater than or equal to the channel delay extension so as to avoid ISI and assure inter-carrier orthogonality. When this assumption is satisfied, the benefits related to CP for communication purpose could also be derived as advantages for passive radar application. By truncating the part of CPs corresponding to the first path, the received signal in the useful duration at k-th subcarrier can be expressed as

$$\boldsymbol{S}_k = \boldsymbol{a}(\theta_1^{\mathrm{c}})c_1\boldsymbol{Q}_k^{\mathrm{T}} + \sum_{n=2}^{M_{\mathrm{c}}}\boldsymbol{a}(\theta_n^{\mathrm{c}})c_n \exp\left(-j2\pi f_k\tau_n^{\mathrm{c}}\right)\boldsymbol{Q}_k^{\mathrm{T}} + \sum_{m=1}^{M_{\mathrm{t}}}\boldsymbol{a}(\theta_m^{\mathrm{t}})\alpha_m \exp\left[-j2\pi\left(f_k - f_m^{\mathrm{D}}\right)\tau_m\right]\boldsymbol{U}_{k,m}^{\mathrm{T}} + \boldsymbol{W}_k \quad (6)$$

where $\boldsymbol{Q}_k = \left[C_{0,k}, C_{1,k}, \cdots, C_{L-1,k}\right]^{\mathrm{T}}$, L is the number of OFDM blocks used as snapshots, and

$$\boldsymbol{U}_{k,m} \approx \left[C_{0,k}, C_{1,k}\exp\left[j2\pi f_m^{\mathrm{D}}T_{\mathrm{s}}\right], \cdots, C_{L-1,k}\exp\left[j2\pi f_m^{\mathrm{D}}T_{\mathrm{s}}(L-1)\right]\right]^{\mathrm{T}} \quad (7)$$

The constant phase rotation approximation within one OFDM block, *i.e.* $\exp\left(j2\pi f_m^{\mathrm{D}}t\right) \approx 1$, $\forall t \in [-T_{\mathrm{cp}}, T_{\mathrm{u}}]$, is applied in Eq. (7), and the $\tau_m < T_{\mathrm{cp}}$ is also assumed. This approximation is satisfied when the product between T_{s} and the Doppler shift f_m^{D} is small compared to unity.

Note that the samples of the clutters at one subcarrier are coherent with each other, whereas target signals are uncorrelated to the clutters due to phase rotation introduced by the Doppler frequency. After merging similar terms, Eq. (6) can be simplified as

$$\boldsymbol{S}_k = \left[\boldsymbol{a}(\theta_1^{\mathrm{c}})c_1 + \sum_{n=2}^{M_{\mathrm{c}}}\boldsymbol{a}(\theta_n^{\mathrm{c}})c_n \exp\left(-j2\pi f_k\tau_n^{\mathrm{c}}\right)\right]\boldsymbol{Q}_k^{\mathrm{T}} + \sum_{m=1}^{M_{\mathrm{t}}}\boldsymbol{a}(\theta_m^{\mathrm{t}})\alpha_m \exp\left[-j2\pi\left(f_k - f_m^{\mathrm{D}}\right)\tau_m\right]\boldsymbol{U}_{k,m}^{\mathrm{T}} + \boldsymbol{W}_k \quad (8)$$

As expected, all the zero-Doppler clutters are integrated into a single term. $\left[\boldsymbol{a}(\theta_1^{\mathrm{c}})c_1 + \sum_{n=2}^{N_{\mathrm{c}}}\boldsymbol{a}(\theta_n^{\mathrm{c}}) \cdot c_n \exp\left(-j2\pi f_k\tau_n^{\mathrm{c}}\right)\right]$ could be viewed as the composite steering vector of clutters. It indicates that only one degree of freedom is required for cancelling the zero-Doppler clutters. Thus the degree of freedom is no longer a limiting factor in subcarrier-based processing. This characteristic indicates that subcarrier-based processing possesses the potential for clutter rejection under SFN configuration in CP-OFDM signal based passive radar. In summary, the diagram of subcarrier-based processing is illustrated in Fig. 2.

3 Novel Characteristics of SSAP

Observing Eq. (8), there are two aspects to distinguish between clutters and target echoes. (1) Clutters are coherent with the transmitted information at each subcarrier, whereas target signals are different due to Doppler frequency. (2) Clutters and target signals have different steering vectors if spatial information is further considered. Thus, when SSAP is adopted, there is something different with conventional SAP as time correlation

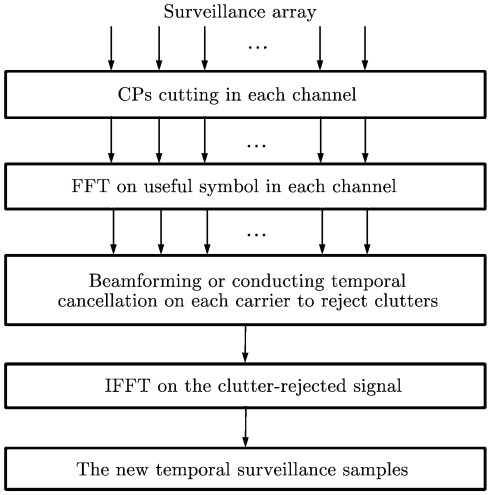

Fig. 2 Flow chart of subcarrier-based processing

is further utilized in SSAP. Corresponding novel characteristics are discussed in this section.

3.1 Doppler response

SSAP utilizes the time correlation among multi-path clutters at each subcarrier in clutter rejection and distinguishes targets from clutters by their Doppler frequency. So the effect of clutter rejection with SSAP could be regarded as a zero-Doppler removal filter. It is conceivable that the target signal with zero Doppler frequency or near zero Doppler frequency is also rejected or weakened. Specifically, we notice that

$$\boldsymbol{U}_{k,m} \approx \boldsymbol{Q}_k \odot \boldsymbol{F}_m \tag{9}$$

where

$$\boldsymbol{F}_m = \left[1, \exp\left[j2\pi f_m^{\mathrm{D}} T_{\mathrm{s}}\right], \cdots, \exp\left[j2\pi f_m^{\mathrm{D}} T_{\mathrm{s}} (L-1)\right]\right]^{\mathrm{T}} \tag{10}$$

and operation "$\odot$" denotes element product.

According to Rayleigh limit criterion, when target Doppler frequency is greater than $1/(LT_s)$, the correlation between the clutters and target signal could be ignored. It is expected that the target signal will not be cancelled with the clutters. This kind of Doppler response provides the basis for the snapshot duration selection.

Specifically, to quantitatively illustrate this response, we exploit the data set acquired in a typical real-life scenario. A synthesized target echo has been injected into the available data, generated as a delayed and Doppler shifted replica data of the reference signal with known input power. Then SSAP has been applied and the output target power has been evaluated by coherent integration. By varying the Doppler frequency (which is normalized to the Doppler resolution to make the results independent on the coherent processing interval) of the injected target and averaging the results over 100 data files, the Doppler response is represented by the Signal-to-Noise Ratio (SNR) gains versus Doppler. As showed in Fig. 3 where the SNR gains has been normalized to the maximum theoretical SNR gain, the SSAP yields a corresponding SNR loss for small Doppler targets. Specifically, the SNR loss could be less than 1.5 dB when target's Doppler is equal to or greater than the Doppler resolution, which is consistent with the above theoretical discussion.

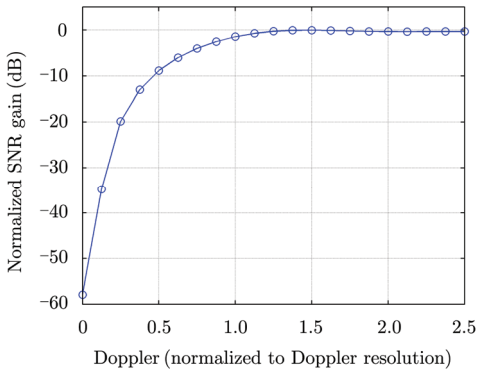

Fig. 3 Doppler response of SSAP

3.2 Unusual main-lobe clutter case

Generally, conventional SAP can not cancel the main-lobe clutter, leading to some blind bearing intervals that correspond to the illuminators. Especially under SFN configuration, these blind bearing intervals may occupy a large proportion of the whole region. Fortunately, SSAP can address the main-lobe clutters to some degree. Because the composite steering vector of the clutters can be different from the scanned steering vector with quite a probability even if some clutters exist in the main lobe. This can be regarded as an additional advantage of SSAP.

Nevertheless, the composite steering vector may cause other effect under subcarrier-based processing. For example, considering the case of two clutters, then the composite steering vector can be expressed as

$$\boldsymbol{u} = \boldsymbol{a}(\theta_1^{\mathrm{c}})c_1 + \boldsymbol{a}(\theta_2^{\mathrm{c}})c_2 \exp\left(-j2\pi f_k \tau_2^{\mathrm{c}}\right) \tag{11}$$

Now we investigate the array response in θ_1^{c} on condition that the main lobe is pointing to θ_2^{c}. Assume the weight vector $\boldsymbol{v}$, then we get

$$\begin{cases} \boldsymbol{v}^{\mathrm{H}} \boldsymbol{a}(\theta_2^{\mathrm{c}}) = 1 \\ \boldsymbol{v}^{\mathrm{H}} \boldsymbol{u} \approx 0 \end{cases} \tag{12}$$

where superscript "H" denotes Hermitian operation.

Substitute Eq. (11) into Eq. (12), we further obtain

$$\boldsymbol{v}^{\mathrm{H}} \boldsymbol{a}(\theta_1^{\mathrm{c}}) \approx -\frac{c_2}{c_1} \exp\left(-j2\pi f_k \tau_2^{\mathrm{c}}\right) \tag{13}$$

Two points should be noted in Eq. (13). (1) The amplitude response in sidelobe clutter azimuth is proportional to the clutter strength ratio. Specifically, the greater the main-lobe to sidelobe

clutter ratio, the higher the amplitude response in sidelobe clutter azimuth. (2) The phase response is a linear function of subcarrier frequency. This linear phase response will cause delay shift of target signal if it does exist in the sidelobe. The shift amount is equal to the delay difference between the main-lobe clutter and sidelobe clutter. Then a peak with new delay may be detected if the strength ratio is proper, which is a false alarm.

The case that considers more clutters will reach similar results. Certainly, the derivation is more difficult so that it have to adopt a reasonable approximation. It can be concluded that, even though the main-lobe clutter could be rejected with SSAP to some degree, false alarms may caused by the target signals in certain azimuths of sidelobe clutters. These false alarms are at its height when main lobe is pointing to the azimuth of the strongest clutters.

This main-lobe clutter case may be alleviated from two respects. (1) Adopt STR instead of SSAP. Temporal processing does not involve main-lobe clutter problem. (2) Appropriate deploy the receiver site to avoid such situation where the area of interest is in the direction of the strongest illuminators.

4 Robustness Investigation

Notice that above explanation about the principle of subcarrier-based processing is based on two basic assumptions, *i.e.* CFO is equal to zero and the channel delay extension is shorter than CP. However, these two assumptions may be violated slightly in real systems. Thus, the sensitivity of subcarrier-based processing to these two factors should be discussed.

4.1 Sensitivity to CFO

When there is residual CFO, *i.e.* $f_{\mathrm{CFO}} \neq 0$, the array signal model is given by

$$\begin{aligned}\boldsymbol{s}'(t) = &\left[\boldsymbol{a}(\theta_1^{\mathrm{c}})c_1 d(t) + \sum_{i=2}^{M_{\mathrm{c}}} \boldsymbol{a}(\theta_i^{\mathrm{c}})c_n d(t-\tau_i^{\mathrm{c}})\right.\\ &\left.+\sum_{m=1}^{M_{\mathrm{t}}} \boldsymbol{a}(\theta_m^{\mathrm{t}})\alpha_m d(t-\tau_m)\exp\left(j2\pi f_m^{\mathrm{D}} t\right)\right]\\ &\cdot\exp\left(j2\pi f_{\mathrm{CFO}} t\right) + \boldsymbol{w}(t)\end{aligned} \tag{14}$$

The approximation of clutters should be cautious as clutters are the components to be rejected. Without loss of generality, we consider one clutter at first, for example, the clutter $d(t-\tau_i^{\mathrm{c}})\cdot\exp\left(j2\pi f_{\mathrm{CFO}} t\right)$. After discretization at the l-th OFDM block, the clutter in the useful symbol conforms to

$$\begin{aligned}d'(n) = &d(lN_{\mathrm{s}} + n - n_i^{\mathrm{c}})\\ &\cdot\exp\left(j2\pi\frac{f_{\mathrm{CFO}}}{f_{\Delta}}n\right)\exp\left(j2\pi f_{\mathrm{CFO}} lT_{\mathrm{s}}\right),\\ &n = 0,1,\cdots,N_{\mathrm{u}}-1\end{aligned} \tag{15}$$

where $t = (lN_{\mathrm{s}} + n)\Delta$, Δ is sampling period, $N_{\mathrm{s}} = T_{\mathrm{s}} f_{\Delta}$ and $N_{\mathrm{u}} = T_{\mathrm{u}} f_{\Delta}$, f_{Δ} is the sampling frequency. Besides, $\tau_i^{\mathrm{c}} = n_i^{\mathrm{c}}\Delta$ is assumed to be the integer multiple sampling periods.

Then clutter information at k-th subcarrier can be expressed as

$$\begin{aligned}D'(k) &= \sum_{n=0}^{N_{\mathrm{u}}-1} d'(n)\exp\left(-j2\pi\frac{k}{N_{\mathrm{u}}}n\right)\\ &= \sum_{n=0}^{N_{\mathrm{u}}-1} d(lN_{\mathrm{s}} + n - n_i^{\mathrm{c}})\exp\left(j2\pi\frac{f_{\mathrm{CFO}}}{f_{\Delta}}n\right)\\ &\quad\cdot\exp\left(-j2\pi\frac{k}{N_{\mathrm{u}}}n\right)\times\exp\left(j2\pi f_{\mathrm{CFO}} lT_{\mathrm{s}}\right)\end{aligned} \tag{16}$$

In addition, we have

$$d(lN_{\mathrm{s}} + n - n_i^{\mathrm{c}}) = \frac{1}{N_{\mathrm{u}}}\sum_{m=0}^{N_{\mathrm{u}}-1} C_{l,m}\exp\left[j2\pi\frac{m}{N_{\mathrm{u}}}\left(n - n_i^{\mathrm{c}}\right)\right] \tag{17}$$

Substitutes Eq. (17) into Eq. (16), then we get

$$\begin{aligned}D'(k) = &\exp\left(j2\pi f_{\mathrm{CFO}} lT_{\mathrm{s}}\right)\sum_{m=0}^{N_{\mathrm{u}}-1}\left[C_{l,m}\exp\left(-j2\pi\frac{m}{N_{\mathrm{u}}}n_i^{\mathrm{c}}\right)\right.\\ &\cdot\sin\left[\pi\left(\frac{f_{\mathrm{CFO}}}{f_{\Delta}} - \frac{k-m}{N_{\mathrm{u}}}\right)N_{\mathrm{u}}\right]\\ &\left/\left[N_{\mathrm{u}}\sin\left[\pi\left(\frac{f_{\mathrm{CFO}}}{f_{\Delta}} - \frac{k-m}{N_{\mathrm{u}}}\right)\right]\right]\right.\\ &\left.\cdot\exp\left(j\pi\left(\frac{f_{\mathrm{CFO}}}{f_{\Delta}} - \frac{k-m}{N_{\mathrm{u}}}\right)(N_{\mathrm{u}}-1)\right)\right]\end{aligned} \tag{18}$$

In Eq. (18), if $f_{\mathrm{CFO}} = 0$, we can arrive at that $D'(k)$ is merely relevant with $C_{l,k}$, which is what subcarrier orthogonality asserts. However, when $f_{\mathrm{CFO}} \neq 0$, $D'(k)$ is the function of transmitted information at all subcarriers, *i.e.* $C_{l,m}$, $m = 0,1,\cdots,N_{\mathrm{u}}-1$. Employing superposition principle, it can be observed that clutters at k-th subcarrier no longer occupy just one degree of freedom, and each

term $C_{l,m}$ seems to occupy one instead. Fortunately, the CFO is usually not large under modern hardware level. It is easy to reach $f_{\mathrm{CFO}}/f_{\Delta}<1/(2N_{\mathrm{u}})$, which means the term related to $C_{l,k}$ is the dominant component of clutter at k-th subcarrier. What we are interested now is that what CFO level can prevent remarkable rejection performance degradation without adding array degree of freedom if SSAP is utilized.

Notice that if the power of the terms related to $C_{l,m}$ $(m=0,\cdots,k-1,k+1,\cdots,N_{\mathrm{u}}-1)$ is lower than noise, it would be reasonable to ignore it with little performance degradation. Furthermore, terms $C_{l,k-1}$ or $C_{l,k+1}$ possess the highest power among these terms. So it only needs to compare the power of terms $C_{l,k-1}$ and $C_{l,k+1}$ with the noise to determine the required CFO level. Specifically, through comparing the reciprocal of Clutter-to-Noise Ratio (CNR) with the amplitude of terms $C_{l,k-1}$ and $C_{l,k+1}$, the required CFO level could be obtained. As the amplitude of terms $C_{l,k-1}$ and $C_{l,k+1}$ are the discrete version of sinc function in accordance with Eq. (18), it can be regarded as the function about $f_{\mathrm{CFO}}N_{\mathrm{u}}/f_{\Delta}$ with great accuracy especially when N_{u} get a relatively large value. Fig. 4 shows the amplitude of the larger one between $C_{l,k-1}$ and $C_{l,k+1}$ versus $f_{\mathrm{CFO}}N_{\mathrm{u}}/f_{\Delta}$. For example, if CNR is 40 dB, it can be derived that the required CFO conforms to $f_{\mathrm{CFO}}N_{\mathrm{u}}/f_{\Delta}<0.01$, i.e. $f_{\mathrm{CFO}}<0.01f_{\Delta}/N_{\mathrm{u}}$. In fact, $f_{\Delta}/N_{\mathrm{u}}$ denotes the Subcarrier Frequency Interval (SFI). So the condition $f_{\mathrm{CFO}}<0.01f_{\Delta}/N_{\mathrm{u}}$ indicates that the CFO should be smaller that 0.01 SFI. Usually the SFI is relative large, for instance, the SFI of 8 MHz mode CMMB signal is about 2.44 kHz, 0.01 SFI means that the required CFO should be smaller than 24.4 Hz. 24.4 Hz CFO is a relative large value which can represent the most cases in practice. So SSAP is not sensitive to CFO.

As for STR, the philosophy behind it is to cancel the component of surveillance sample that are coherent with the reference sample $C_{l,k}$ at k-th subcarrier. Since the terms related to $C_{l,m}$ $(m=0,\cdots,k-1,k+1,\cdots,N_{\mathrm{u}}-1)$ in Eq. (18) is not correlated with reference sample $C_{l,k}$, so these terms will sustain after STR, constituting interference for target detection. Thus, the CFO requirement for SSAP should be also satisfied in STR. In addition, there is another phase factor term caused by CFO in Eq. (18), i.e. $\exp(j2\pi\cdot f_{\mathrm{CFO}}lT_{\mathrm{s}})$. The phase factor will lead to correlation loss between the term related to $C_{l,k}$ in surveillance signal and reference sample.

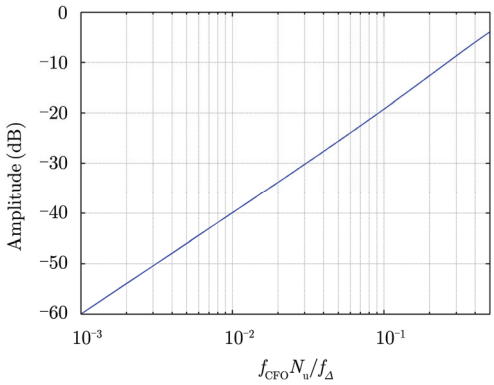

Fig. 4 Amplitude of the larger one between $C_{l,k-1}$ and $C_{l,k+1}$ versus $f_{\mathrm{CFO}}N_{\mathrm{u}}/f_{\Delta}$

Record the term $C_{l,k}\exp(j2\pi f_{\mathrm{CFO}}lT_{\mathrm{s}})$ in surveillance signal as

$$\boldsymbol{B}_k=\left[C_{0,k},C_{1,k}\exp(j2\pi f_{\mathrm{CFO}}T_{\mathrm{s}}),\cdots,C_{L-1,k}\exp(j2\pi f_{\mathrm{CFO}}T_{\mathrm{s}}(L-1))\right]^{\mathrm{T}} \tag{19}$$

where the complex amplitude is ignored for brevity.

Applying orthogonal projection principle, the residual sample conforms to

$$\boldsymbol{S}_{\mathrm{res}}=\boldsymbol{B}_k-\boldsymbol{Q}_k\left(\boldsymbol{Q}_{\mathrm{k}}^{\mathrm{H}}\boldsymbol{Q}_k\right)^{-1}\boldsymbol{Q}_{\mathrm{k}}^{\mathrm{H}}\boldsymbol{B}_k \tag{20}$$

Assume the module of $C_{l,k}$ is a constant, then the residual power ratio can be expressed as

$$\eta=\frac{\boldsymbol{S}_{\mathrm{res}}^{\mathrm{H}}\boldsymbol{S}_{\mathrm{res}}}{\boldsymbol{B}_k^{\mathrm{H}}\boldsymbol{B}_k}=1-\left|\frac{\sin(\pi f_{\mathrm{CFO}}T_{\mathrm{s}}L)}{L\sin(\pi f_{\mathrm{CFO}}T)}\right|^2 \tag{21}$$

Similarly, the residual power ratio versus $f_{\mathrm{CFO}}T_{\mathrm{s}}L$ is presented in Fig. 5. It can be observed that the required CFO should satisfy $f_{\mathrm{CFO}}T_{\mathrm{s}}L<0.0055$ $(i.e.\ f_{\mathrm{CFO}}<0.0055/(T_{\mathrm{s}}L))$ if 40 dB rejection is needed. $1/(T_{\mathrm{s}}L)$ denotes the frequency resolution as $T_{\mathrm{s}}L$ is the processing duration. Thus, the required CFO level is directly related to the frequency resolution, which is a tougher restriction compared with the SSAP case. For instance, if the processing duration is 25 ms, then required CFO should be smaller than 0.22 Hz. Apparently, STR is more sensitive to CFO. In practice, the transmitters

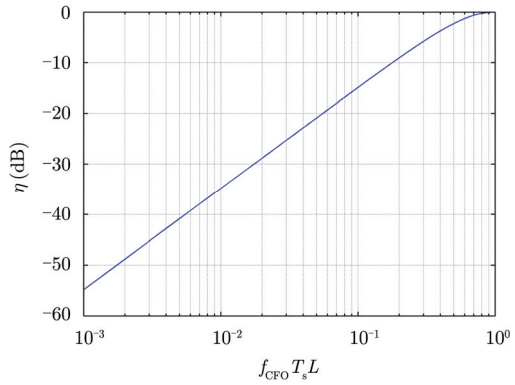

Fig. 5 Residual power ratio versus $f_{\mathrm{CFO}}T_{\mathrm{s}}L$ in STR

in SFN adopt GPS technique to achieve frequency and time synchronization. Thus, to employ STR method for clutter rejection under SFN configation, it is necessary to adopt GPS in the receiving terminal and to be supplemented with CFO estimation and compensation methods.

In fact, if the module of $C_{l,k}$ is not a constant, Eq. (21) reflects the mean level of clutter rejection performance. Thus, above discussion also applies to CFO sensitivity analysis of other types of temporal approaches.

4.2 Excessive channel delay extension

The assumption that CP is greater than or equal to the channel delay extension could not always hold. This is really true from a radar point of view, especially in SFN configuration, and will be substantiated in the successive experimental results. For convenience, we name the clutter whose delay exceeds the CP as far clutter and the clutter whose delay is less than or equal to the CP as near clutter. Even though the far clutters pose little threat to the correct decoding for communication purpose as they are usually 10–40 dB below the direct-path signal or other strong near clutters, they indeed cause trouble for radar detection since they could still be much stronger than the reflected target echoes. Thus, further discussion should be conducted to investigate the robustness of SSAP to far clutters. Without loss of generality, here we consider the case of one far clutter. The received signal conforms to

$$\begin{aligned}\boldsymbol{s}(t)=&\boldsymbol{a}(\theta_1^{\mathrm{c}})c_1d(t)+\sum_{n=2}^{M_{\mathrm{c}}}\boldsymbol{a}(\theta_n^{\mathrm{c}})c_nd(t-\tau_n^{\mathrm{c}})\\&+\boldsymbol{a}(\theta_1^{\mathrm{fc}})c_1^{\mathrm{f}}d(t-\tau_{\mathrm{c}})+\sum_{m=1}^{M_{\mathrm{t}}}\boldsymbol{a}(\theta_m^{\mathrm{t}})\alpha_md(t-\tau_m)\\&\cdot\exp\left(j2\pi f_m^{\mathrm{D}}t\right)+\boldsymbol{w}(t)\end{aligned}\tag{22}$$

where the first and second terms denote near clutter and the third term denotes far clutter.

The distinction between far clutters and near clutters can be clearly figured out from Fig. 6. If far clutters exist, there are signals from both the current OFDM block and the previous OFDM block in the selected useful symbol interval $[0,T_{\mathrm{u}}]$. So the far clutter can be written as

$$d(t-\tau_{\mathrm{c}})=x_1(t)+x_2(t),\ 0\le t\le T_{\mathrm{u}}\tag{23}$$

where

$$x_1(t)=\begin{cases}\sum_{k=0}^{K-1}C_{-1,k}\psi'_{-1,k}(t+T_{\mathrm{u}}+T_{\mathrm{cp}}-\tau_{\mathrm{c}}),\\\qquad 0\le t<\tau_{\mathrm{c}}-T_{\mathrm{cp}}\\0,\quad \tau_{\mathrm{c}}-T_{\mathrm{cp}}\le t\le T_{\mathrm{u}}\end{cases}\tag{24}$$

and

$$x_2(t)=\begin{cases}0, & 0\le t<\tau_{\mathrm{c}}-T_{\mathrm{cp}}\\\sum_{k=0}^{K-1}C_{0,k}\psi'_{0,k}(t-\tau_{\mathrm{c}}), & \tau_{\mathrm{c}}-T_{\mathrm{cp}}\le t\le T_{\mathrm{u}}\end{cases}\tag{25}$$

At this moment the subcarrier samples of the far clutter $d(t-\tau_{\mathrm{c}})$ are not totally correlated with the ones of the near clutters. Specifically, the subcarrier samples of component $x_2(t)$ are partially correlated with the near clutters and the subcarrier samples of component $x_1(t)$ are uncorrelated with the near clutters.

To gain insight into the subcarrier-based processing in the case where there exist far clutters, we divide the component $x_2(t)$ at k-th subcarrier into two parts

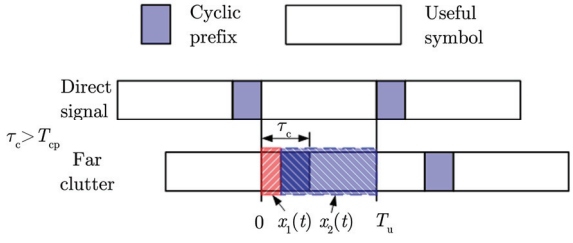

Fig. 6 The illustration of far clutter

$$\boldsymbol{X}_2[k]=\frac{T_{\mathrm{u}}+T_{\mathrm{cp}}-\tau_{\mathrm{c}}}{T_{\mathrm{u}}}\boldsymbol{Q}_k^{\mathrm{T}}\exp\left(-j2\pi f_k\tau_{\mathrm{c}}\right)+\boldsymbol{X}_{\mathrm{r}}[k] \quad (26)$$

where the first term $\left[\left(T_{\mathrm{u}}+T_{\mathrm{cp}}-\tau_{\mathrm{c}}\right)/T_{\mathrm{u}}\right]\boldsymbol{Q}_k^{\mathrm{T}}\cdot\exp\left(-j2\pi f_k\tau_{\mathrm{c}}\right)$ is totally correlated with the one of near clutter while the second one $\boldsymbol{X}_{\mathrm{r}}[k]$ contributed by spectrum leakage is uncorrelated with near clutter. Usually the strength of the second one is much below the first one. Then the k-th subcarrier samples conforms to

$$\begin{aligned}\boldsymbol{S}_k=&\left[\boldsymbol{a}(\theta_1^{\mathrm{c}})c_1+\sum_{n=2}^{M_{\mathrm{c}}}\boldsymbol{a}(\theta_n^{\mathrm{c}})c_n\exp\left(-j2\pi f_k\tau_n^{\mathrm{c}}\right)\right.\\&\left.+\boldsymbol{a}(\theta_1^{\mathrm{fc}})c_1^{\mathrm{f}}\frac{T_{\mathrm{u}}+T_{\mathrm{cp}}-\tau_{\mathrm{c}}}{T_{\mathrm{u}}}\exp\left(-j2\pi f_k\tau_{\mathrm{c}}\right)\right]\boldsymbol{Q}_k^{\mathrm{T}}\\&+\boldsymbol{a}(\theta_1^{\mathrm{fc}})c_1^{\mathrm{f}}\left[\boldsymbol{X}_1[k]+\boldsymbol{X}_{\mathrm{r}}[k]\right]+\sum_{m=1}^{M_{\mathrm{t}}}\boldsymbol{a}(\theta_m^{\mathrm{t}})\alpha_m\\&\cdot\exp\left[-j2\pi\left(f_k-f_m^{\mathrm{D}}\right)\tau_m\right]\boldsymbol{U}_{k,m}^{\mathrm{T}}+\boldsymbol{W}_k \quad (27)\end{aligned}$$

This recombination of near clutter and far clutter gives us a new perspective to the spatial property of the clutters. First, the degree of freedom required for clutter rejection in subcarrier domain will not exceed the one in time domain. Second, even though one additional degree of freedom may be needed for a far clutter, the power distribution on each steering vector has changed. Note that the component $x_2(t)$ is generally the dominant component of far clutter as long as the exceeded delay is small compared to the useful symbol duration. It indicates that $c_1^{\mathrm{f}}\left[\boldsymbol{X}_1[k]+\boldsymbol{X}_{\mathrm{r}}[k]\right]$ only accounts for a small fraction of the energy of far clutter in the subcarrier domain. In extreme cases where the power of $c_1^{\mathrm{f}}\left[\boldsymbol{X}_1[k]+\boldsymbol{X}_{\mathrm{r}}[k]\right]$ is lower than the thermal noise, this term can merge into noise with little deterioration of the detection performance. Two such cases can occur in practice. (1) The exceeded delay is very short. (2) The far clutters have low power. Certainly, even these two conditions do not hold, adding array elements can effectively rejected the far clutters. As there is usually a small amount of strong far clutters thanks to the networking signal structure considerations in communication, relatively small array can achieve desirable clutter rejection under SFN configuration with SSAP. Thus, SSAP is robust to far clutters.

As for STR, $c_1^{\mathrm{f}}\left[\boldsymbol{X}_1[k]+\boldsymbol{X}_{\mathrm{r}}[k]\right]$ is the residual component of far clutters that can not be rejected with STR. So STR possesses slightly lower performance with respect to far clutters compared with SSAP. However, the influence of far clutters is a gradual process. No "threshold effect" exists. In this sense, STR still possesses robustness to far clutters to some degree.

5 Simulation and Real-life Data Results

5.1 Simulations about the robustness

To verify the theoretical analyses about the robustness, several simulations are conducted. The main parameters involving in the simulations are listed in Tab. 1.

Tab. 1 Parameters list of the simulations

Order	Parameters' value
Shared parameters	Direct signal: delay=0, DNR=35 dB, DOA= $-30°$; Near clutter 1: delay= 120Δ , CNR=30 dB, DOA= $-25°$; Near clutter 2: delay= 240Δ , CNR=30 dB, DOA= $-20°$; Near clutter 3: delay= 360Δ , CNR=30 dB, DOA= $-10°$; Target echo: delay= 200Δ , SNR= -20 dB, DOA= $0°$, Doppler= $10/(T_{\mathrm{s}}L)$; L=53.
Simulation 1	Array: 2 elements, element spacing=half wavelength; $f_{\mathrm{CFO}}=(0.005:0.005:0.05)f_{\Delta}/N_{\mathrm{u}}$; SSAP.
Simulation 2	$f_{\mathrm{CFO}}=(0.005:0.005:0.05)/(T_{\mathrm{s}}L)$; STR.
Simulation 3	Array: 2 elements, element spacing=half wavelength; Far clutter: exceeded delay= $(0:5:45)\Delta$, CNR=10, 20 dB, DOA= $30°$; SSAP, $f_{\mathrm{CFO}}=0$.
Simulation 4	Array: 2 elements, element spacing=half wavelength; Far clutter: exceeded delay= $(0:50:450)\Delta$, CNR=5, 10 dB, DOA= $30°$; SSAP, $f_{\mathrm{CFO}}=0$.
Simulation 5	Array: 3 elements ULA, element spacing=half wavelength; Far clutter: exceeded delay= $(0:50:450)\Delta$, CNR=30 dB, DOA= $30°$; SSAP, $f_{\mathrm{CFO}}=0$.

Note: The DOA (Direction Of Arrival) is relative to boresight of the ULA (Uniform Linear Array) with positive defined in clockwise. The duration of CP is 512Δ and the duration of useful symbol is 4096Δ . If the exceeded delay is 10Δ , it means that the total delay is 522Δ . The SNR of the target echo is the value before coherent integration. The theoretical gain of matched filtering is 52 dB.

For each considered case, 100 independent simulations are performed. Simulation 1 and Simulation 2 are conducted to verify the discussion about sensitivity to CFO. The results are shown in Fig. 7(a) where the CFO of SSAP case is normalized to f_Δ / N_u and the CFO of STR case is normalized to $1/(T_s L)$. As expected, the SNR of both cases decreases with the increase of normalized CFO. With respect to SSAP, when CFO reach $0.05 f_\Delta / N_u$, the SNR loss is about 8 dB, which is consistent with the theoretical analysis as shown in Fig. 4. As for STR, when CFO arrive at $0.05/(T_s L)$, the SNR loss is about 12 dB, which is slightly lower than theoretical value (about 14 dB) since the residual power of the clutter is not totally equal to Gauss white noise. On the whole, the simulations confirm the theoretical analysis about the CFO sensitivity.

In the Simulation 3, we want to investigate how much exceeded delay will have impact on the clutter suppression performance without adding extra degree of freedom. The results are shown in Fig. 7(b). When the exceeded delay is small, specifically, 20Δ for 20 dB CNR and more than 50Δ for 10 dB CNR, one degree of freedom is enough to cancel the clutters with SNR loss less than 1 dB in the considered case.

In the Simulation 4, the influence of CNR on the clutter rejection performance is researched and the results are presented in Fig. 7(c). Concluding from the results, we get that the output SNR decline gently versus exceeded delay with CNR equal to 5 dB and 10 dB. The results of Simulation 3 and Simulation 4 validate the discussed extreme cases following Eq. (27).

In the Simulation 5, the results (as illustrated in Fig. 7(c)) show that adding a degree of freedom can effectively suppresses a strong far clutter.

Combining the theoretical and simulation results, it can be concluded that the SSAP is not sensitive to CFO whereas STR is sensitive to CFO. In addition, SSAP is robust to far clutters. When the exceeded delay is short or the far clutters are weak, little deterioration can be observed without

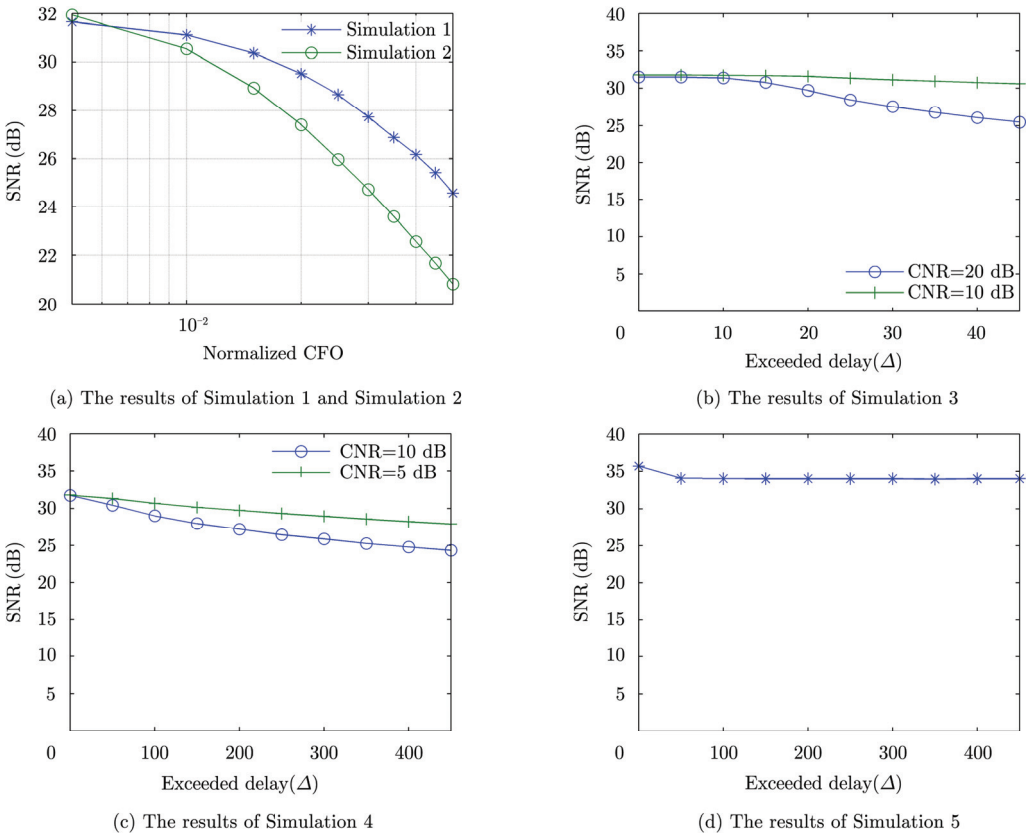

(a) The results of Simulation 1 and Simulation 2

(b) The results of Simulation 3

(c) The results of Simulation 4

(d) The results of Simulation 5

Fig. 7 The simulation results about the robustness of subcarrier-based processing

increasing the degree of freedom. If this case does not hold, adding array elements can effectively handle the far clutters. Therefore small array can achieve desirable clutter rejection in the complex environment with SSAP as there is usually a small amount of strong far clutters.

5.2 Real-life data results

To demonstrate the validity of subcarrier-based processing in practical environment, real-life data is used for evaluation. The real-life data is acquired by Wuhan University under typical airborne target detection scenario. The ARD (Amplitude Range-Doppler) map before clutter rejection is illustrated in Fig. 8(a). The ARD maps have been normalized to the maximum amplitude. In Fig. 8(a), the strong peak appearing at zero range and zero velocity is corresponding to the direct signal transmitted by the nearest illuminator. The zero-Doppler components are the contribution of multipath signals. Note that a few strong far clutters can also be observed. The target returns are masked by the pedestal floor of the strong clutters. Fig. 8(b) shows the result after clutter rejection with SSAP. As is apparent, the clutters at zero Doppler are effectively rejected and the targets can be clearly observed.

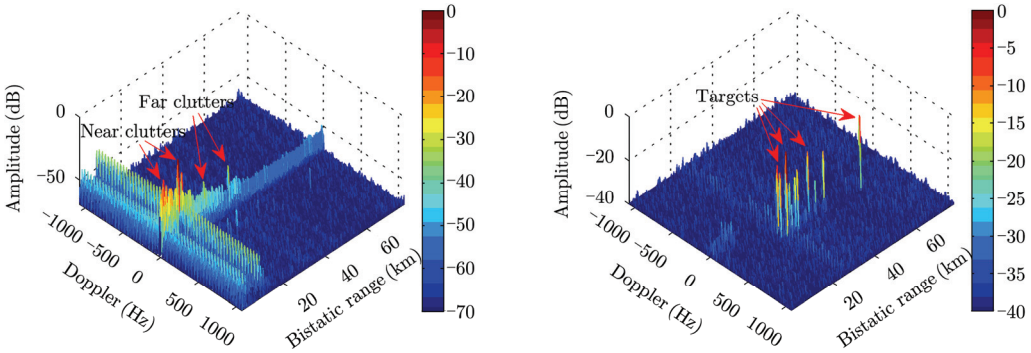

(a) The ARD map without clutter rejection

(b) The ARD map after clutter rejection with SSAP

Fig. 8 ARD results of real-life data

6 Conclusions and Future Work

This paper has investigated the principle, characteristics and robustness of subcarrier-based processing. Both SSAP and STR are brought into its theoretical frame. Theoretical and simulation results show that subcarrier-based processing can save degree of freedom since clutters at each subcarrier are coherent with each other. This coherence causes several novel features for subcarrier-based processing. The Doppler response of SSAP demonstrates its zero-Doppler removal characteristic. And the unusual main-lobe clutter case of SSAP indicates that it may lead to false alarms at certain bearings although it can reject the main-lobe clutters to some degree. In terms of robustness, SSAP is robust to CFO and far clutters, whereas STR is comparatively more sensitive to these factors. Taking CFO for example, for 40 dB clutter rejection requirement, the required CFO level for SSAP is about 0.01 SFI, whereas for STR the level is about 0.0055 Doppler resolutions. These theoretical conclusions are confirmed by simulations. And the real-life processing results reveal a good performance. It indicates that subcarrier-based processing is a perspective approach for clutter rejection in CP-OFDM signal based passive radar. Certainly, there remain some issues to be further considered, mainly including the sidelobe false alarm problem in main-lobe clutter case. How to deploy the receivers or appropriately combine the STR will be the key considerations.

References

[1] Griffiths H D and Long N R W. Television based bistatic radar[J]. *IEE Proceedings-F, Communications, Radar and Signal Processing*, 1986, 133(7): 649–657.

[2] Howland P E. Target tracking using television-based bistatic radar[J]. *IEE Proceedings-Radar Sonar and Navigation*, 1999, 146(3): 166–174.

[3] Thomas J M, Baker C J, and Griffiths H D. HF passive bistatic radar potential and applications for remote sensing[C]. New

Trends for Environmental Monitoring Using Passive Systems, Hyeres, French Riviera, Oct. 14–17, 2008: 1–5.

[4] Kuschel H and O'Hagan D. Passive radar from history to future[C]. International Radar Symposium (IRS), Vilnius, Lithuania, June 16–18, 2010: 1–4.

[5] Berger Christian R, Bruno Demissie, Jörg Heckenbach, *et al.*. Signal processing for passive radar using OFDM waveforms[J]. *IEEE Journal of Selected Topics in Signal Processing*, 2010, 4(1): 226–238.

[6] Wan Xian-rong. An overview on development of passive radar based on the low frequency band digital broadcasting and TV signals[J]. *Journal of Radars*, 2012, 1(2): 109–123.
万显荣. 基于低频段数字广播电视信号的外辐射源雷达发展现状与趋势[J]. 雷达学报, 2012, 1(2): 109–123.

[7] Howland P. Editorial: passive radar systems[J]. *IEE Proceedings-Radar Sonar and Navigation*, 2005, 152(3): 105–106.

[8] Special issue on passive radar (Part I)[J]. *IEEE Aerospace and Electronic Systems Magazine*, 2012, 27(10): 5–59.

[9] Special issue on passive radar (Part II)[J]. *IEEE Aerospace and Electronic Systems Magazine*, 2012, 27(11): 4–55.

[10] Coleman C J and Yardley H. Passive bistatic radar based on target illuminations by digital audio broadcasting[J]. *IET Radar*, *Sonar & Navigation*, 2008, 2(5): 366–375.

[11] Capria A, Petri D, Martorella M, *et al.*. DVB-T passive radar for vehicles detection in urban environment[C]. IEEE Geoscience and Remote Sensing Symposium(IGARSS), July 25–30, 2010: 3917–3920.

[12] O'Hagan D W, Capria A, Petri D, *et al.*. Passive bistatic radar (PBR) for harbour protection applications[C]. IEEE Radar Conference, 2012: 446–450.

[13] Yi Jian-xin, Wan Xian-rong, Fang Liang, *et al.*. Coherent integration implementation for China mobile multimedia broadcasting based passive radar with nonuniform sampling[J]. *Journal of Electronics & Information Technology*, 2012, 34(11): 2648–2653.
易建新, 万显荣, 方亮, 等. 中国移动多媒体广播外辐射源雷达相干积累的非均匀采样实现[J]. 电子与信息学报, 2012, 34(11): 2648–2653.

[14] Colone Fabiola, Falcone Paolo, Bongioanni Carlo, *et al.*. WiFi-based passive bistatic radar: data processing schemes and experimental results[J]. *IEEE Transactions on Aerospace and Electronic Systems*, 2012, 48(2): 1061–1079.

[15] Zhao Zhi-xin, Wan Xian-rong, Zhang De-lei *et al.*. An experimental study of HF passive bistatic radar via hybrid sky-surface wave mode[J]. *IEEE Transactions on Antennas and Propagation*, 2013, 61(1): 415–424.

[16] Poullin Dominique and Flecheux Marc. Passive 3D tracking of low altitude targets using DVB (SFN Broadcasters)[J]. *IEEE Aerospace and Electronic Systems Magazine*, 2012, 27(11): 36–41.

[17] Colone F, O'Hagan D W, Lombardo P, *et al.*. A multistage processing algorithm for disturbance removal and target detection in passive bistatic radar[J]. *IEEE Transcations on Aerospace and Electronic Systems*, 2009, 45(2): 698–722.

[18] Palmer J E and Searle S J. Evaluation of adaptive filter algorithms for clutter cancellation in passive bistatic radar[C]. IEEE Radar Conference, Atlanta, GA, May 7–11, 2012: 493–498.

[19] Fabrizio G, Colone F, Lombardo P, *et al.*. Adaptive beamforming for high-frequency over-the-horizon passive radar[J]. *IET Radar*, *Sonar & Navigation*, 2009, 3(4): 384–405.

[20] Tao R, Wu H Z, and Shan T. Direct-path suppression by spatial filtering in digital television terrestrial broadcasting-based passive radar[J]. *IET Radar*, *Sonar & Navigation*, 2010, 4(6): 791–805.

[21] Poullin D. Passive detection using digital broadcasters (DAB, DVB) with COFDM modulation[J]. *IEE Proceedings-Radar Sonar and Navigation*, 2005, 152(3): 143–152.

[22] Zhao Zhi-xin, Wan Xian-rong, Shao Qi-hong, *et al.*. Multipath clutter suppression by spatial filtering on each carrier in DRM-based passive radar[J]. *Journal of Huazhong University of Science and Technology(Natural Science Edition)*, 2012, 40(3): 13–17.
赵志欣, 万显荣, 邵启红, 等. DRM 无源雷达多径杂波的分载波空域抑制[J]. 华中科技大学学报(自然科学版), 2012, 40(3): 13–17.

[23] Zhao Zhi-xin, Wan Xian-rong, Shao Qi-hong, *et al.*. Multipath clutter rejection for digital radio mondiale-based HF passive bistatic radar with OFDM waveform[J]. *IET Radar*, *Sonar & Navigation*, 2012, 6(9): 867–872.

Yi Jian-xin was born in Hunan, China in 1989. He received the B.E. degree in 2011 from Wuhan University, China. He is now a doctoral candidate of Wuhan University. His paper won the 12th China radar annual conference outstanding paper first prize in 2012. His main area of interests is in signal processing of passive radar and over-the-horizon radar.

Wan Xian-rong was born in Hubei, China in 1975. He received the B.E. degree in former Wuhan Technical University of Surveying and Mapping in 1997 and Ph.D. degree in Wuhan University in 2005, China, respectively. He is now a professor and Ph.D. candidate supervisor with Wuhan University. Recent years he has hosted and participated in more than ten national research projects, and published more than 60 academic papers. His main research interests include design of new radar system such as passive radar, over-the-horizon radar, and array signal processing.

Zhao Zhi-xin was born in Hubei, China in 1986. She received the B.E. degree in 2008 from Wuhan University, China. She is now a doctoral candidate of Wuhan University. Her main area of interests is in signal processing of over-the-horizon radar and passive radar.

Cheng Feng obtained the B.E. degree in electronic engineering in 1998 and Ph.D. degree in radio physics in 2006, respectively, both from Wuhan University, China. His main research interests are radar signal processing, radio ocean remote sensing and radar software engineering.

Ke Heng-yu was born in Hubei, China in 1957. He received Ph.D. degree from Wuhan University in 1996. He is now a professor and Ph.D. candidate supervisor with Wuhan University. His main research interests include electromagnetic radiation and scattering, HF radar ocean remote sensing, radio propagation and antenna.